

Raman study of phase transitions in ion-implanted and Q -switched neodymium-doped yttrium aluminum garnet laser annealed silicon

A. K. Shukla and K. P. Jain

Laser Technology Research Programme, Indian Institute of Technology, New Delhi-110016, India

(Received 20 October 1986)

Dynamic behavior of the abrupt crystalline-to-amorphous (c - a) transition in the ion-implantation process and the amorphous-to-crystalline (a - c) transition in Q -switched neodymium-doped yttrium aluminum garnet laser annealing are studied by use of light scattering. Excess internal energy and excess configurational entropy required for the abrupt c - a transition are invoked to calculate the threshold fluence of implanted species. It is observed that the threshold power density of pulse-laser annealing for recrystallization depends strongly upon the coupling of light to a given thickness of implanted silicon.

INTRODUCTION

Ion-implantation in semiconductors,¹⁻³ which provides an understanding of physical phenomena involved in the formation of the amorphous state, has opened new possibilities of doping. High-energy impurity ions produce radiation damage which results in both compositional and topological disorder.^{3,4} Ion implantation above certain doses induces the implanted material to become amorphous. The crystalline-amorphous (c - a) transition in silicon prepared by various techniques such as glow discharge and sputtering⁵⁻¹⁰ has been reported. Raman scattering is used here to understand the underlying physical phenomena involved in the abrupt c - a transition after ion implantation. It is of basic interest to determine the extent to which crystalline or microcrystalline state is no longer thermodynamically stable with respect to the amorphous phase. Light scattering of disordered solids which has been discussed at length,^{3,5,6} reveals two bands at 160 and 480 cm^{-1} corresponding to the density of states in the acoustic and optical branches of silicon. The coherence length, which basically reflects spatial correlations of atomic displacements of normal modes, varies from very large distances in an ideal crystal much greater than the wavelength of light to a few angstroms in a highly disordered solid.¹¹

Pulse-laser annealing (PLA) of ion-implanted silicon^{2,4,12,13} has been successfully used to repair radiation damage. Many authors have invoked the epitaxial recrystallization of implanted silicon on crystalline substrate during PLA. A number of questions regarding threshold power density of PLA are yet to be resolved. The dynamic behavior of laser annealing using various power densities to induce amorphous-to-crystalline (a - c) transitions which have been studied using techniques such as ion backscattering, electron diffraction, and electrical measurements,^{2,12,13} is studied systematically here by Raman spectroscopy. The threshold power density required for recrystallization of ion-implanted silicon is investigated here as a function of dose of implanted impurity and wavelength of light used in PLA.

Light scattering is one of the most powerful methods to

study a - c and c - a transitions.^{3,4} This is done by investigating a broad band at 470 cm^{-1} characteristic of the disordered state and a narrow peak at 520.5 cm^{-1} of crystalline structure corresponding to zone-center phonons (ZCP). Furthermore, Raman spectrum of crystalline Si (c -Si) reveals broad bands of two-phonon combination modes⁴ around 300, 620, and 950 cm^{-1} corresponding to zone-edge phonons (ZEP). Zone-center phonons reflect their sensitivity to disorder in crystalline silicon by an asymmetry of the one-phonon mode as well as anharmonic effects.¹⁴⁻¹⁶

In this paper, we present a systematic study of the c - a transition in the ion-implantation process and the a - c transition in the PLA using Raman spectroscopy. On the basis of thermodynamic arguments, the threshold fluences of various implanted species are calculated for abrupt the c - a transition in the ion-implantation process.

EXPERIMENTAL PROCEDURES AND RESULTS

Raman scattering experiments of ion implanted and PLA silicon were performed in the backscattering geometry at room temperature using various lines of an argon-ion laser, a Ramanor double monochromator and photon-counting electronics. Silicon $\langle 100 \rangle$ samples were ion implanted with 100 keV As^+ , 50 keV B^+ , and 50 keV P^+ to doses ranging from 10^{12} to 10^{15} ions/ cm^2 . Phosphorous-implanted samples were irradiated with a Q -switched neodymium-doped yttrium aluminum garnet (Nd:YAG) laser ($\lambda = 1.06 \mu\text{m}$) having a pulse duration of 130 nsec and a repetition rate of 1 kHz. The beam spot had a $1/e$ diameter of 100 μm . The sample was vacuum held on a microprocessor-controlled X Y positioning table which was moved at the speed of 2 mm/sec in steps of 10 μm . Power densities (ϕ) used for PLA were 28–65 MW/cm^2 . The sample was stepped to produce a continuously overlapped region of $5 \times 3 \text{ mm}^2$. Laser irradiation was also performed with a frequency-doubled Nd:YAG laser ($\lambda = 0.53 \mu\text{m}$) having a pulse duration of 130 nsec and a repetition rate of 1 kHz.

Figure 1 shows Raman spectra of silicon implanted with 50 keV P^+ to a fluence (f) ranging from 10^{12} to 10^{15}

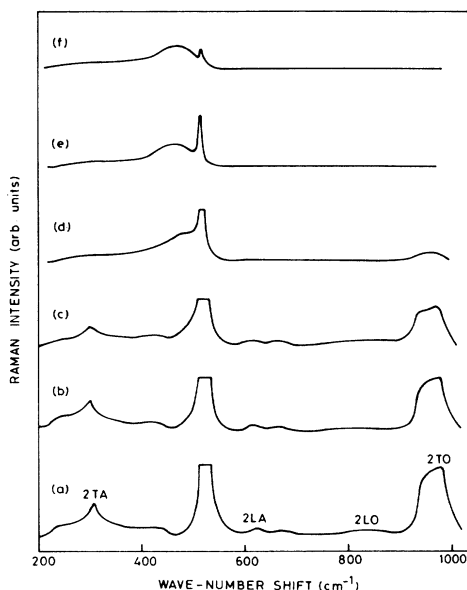


FIG. 1. Room-temperature backscattering Raman spectra with 514.5-nm laser line. (a) Spectrum of pure silicon; (b), (c), (d), (e), and (f) spectra of silicon samples implanted with P^+ to the fluences of 10^{12} , 10^{14} , 3×10^{14} , 5×10^{14} , and 10^{15} ions/cm², respectively. The spectra are arbitrarily cut off at the top of the one-phonon line to focus the attention on second-order spectra.

ions/cm². Below the fluence of 3×10^{14} ions/cm², Raman spectra of implanted silicon with diminished oscillator strength of two phonon modes are quite similar to the reference spectrum of unimplanted silicon as depicted in Figs. 1(a), 1(b), and 1(c). An abrupt transition from crystalline state to amorphous state is observed in Figs. 1(d), 1(e), and 1(f) as the fluence is increased beyond 3×10^{14} ions/cm². Raman spectra of Figs. 1(e) and 1(f) show the formation of amorphous silicon.³ In addition to the usual broad peak (~ 470 cm⁻¹) of amorphous silicon, there is a crystalline peak at 518 and 1000 cm⁻¹ as shown in Fig. 1(d).³ One can note in Figs. 1(d)–1(f) that there is a relatively quick disappearance of the two-phonon scattering (900–1000 cm⁻¹) for a small increase of fluence above 3×10^{14} ions/cm², indicating that the short-wavelength phonons (zone-edge phonons) abruptly disappear. However,

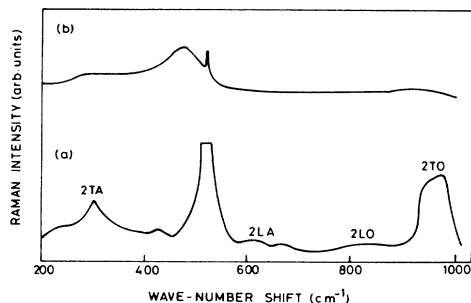


FIG. 2. Room-temperature backscattering Raman spectra with 514.5-nm laser line. (a) Spectrum of a silicon sample implanted with B^+ to a fluence of 10^{15} ions/cm²; (b) spectrum of silicon implanted with As^+ to a fluence of 10^{14} ions/cm².

er, the long-wavelength phonon (~ 518 cm⁻¹) does not disappear abruptly. Softening of long-wavelength phonon from 520 cm⁻¹ (i.e., crystalline silicon) to 518 cm⁻¹ indicates the presence of microcrystals in the amorphous matrix.³

Figure 2(b) shows the Raman spectrum of silicon implanted with 100 keV As^+ to a fluence of 10^{14} ions/cm². It should be noted that Raman spectrum of amorphous silicon which appears at $f = 3 \times 10^{14}$ ions/cm² for P^+ implantation as shown in Fig. 1(d), appears at $f = 10^{14}$ ions/cm² for As^+ implantation in Fig. 2(b). In contrast to the implantation with As^+ and P^+ , Fig. 2(a) shows the Raman spectrum of crystalline silicon at $f = 10^{15}$ ions/cm² using 50 keV B^+ as implanted species. These observations are consistent with the fact that the fluence at which an abrupt transition from crystalline-silicon phase to amorphous-silicon phase takes place decreases with the increase of mass of implanted species.

Figure 3 shows the a - c transition in the Raman spectra of silicon implanted with 50 keV P^+ to a fluence of 3×10^{14} ions/cm² and then annealed with various power densities (ϕ) of Q -switched Nd:YAG laser ($\lambda = 0.53$ μ m). One can see that two-phonon combination (TPC) modes have recovered completely after PLA with $\lambda = 0.53$ μ m and with a power density of 50 MW/cm² in comparison with 55 MW/cm² as shown in Figs. 3(b) and 3(c). The corresponding spectra of PLA with $\lambda = 1.06$ μ m are shown in Fig. 4 indicating that the threshold power density for complete recovery of TPC modes lies between 55 and 65 MW/cm². It should be noted that TPC modes do not recover completely at power density of 55 MW/cm² in PLA with $\lambda = 1.06$ μ m in contrast to PLA with $\lambda = 0.53$ μ m as shown in Figs. 4(b) and 3(c). That means that threshold power density of PLA with $\lambda = 1.06$ μ m for recovery of crystallinity is greater than that of PLA with $\lambda = 0.53$ μ m.

Pulse-laser annealing with $\lambda = 0.53$ μ m and $\lambda = 1.06$ μ m using various power densities of silicon implanted

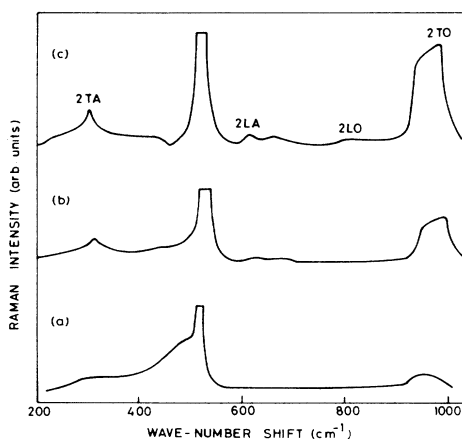


FIG. 3. Room-temperature backscattering Raman spectra with 514.5-nm laser line. (a) Spectrum of a silicon sample implanted with P^+ to a fluence of 3×10^{14} ions/cm². PLA with $\lambda = 0.53$ μ m is done on same implanted sample using power densities of 50 and 55 MW/cm² in (b) and (c), respectively.

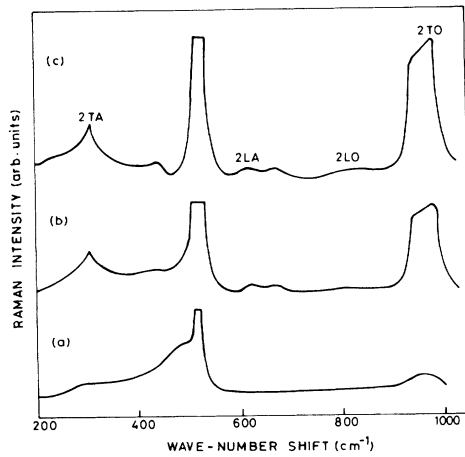


FIG. 4. Room-temperature backscattering Raman spectra with 514.5-nm laser line. (a) Spectrum of a silicon sample implanted with P^+ to a fluence of 3×10^{14} ions/cm². PLA with $\lambda = 1.06 \mu\text{m}$ is done on same implanted sample using power densities of 55 and 65 MW/cm² in (b) and (c), respectively.

with 50 keV P^+ to a fluence of 10^{15} ions/cm² are shown in Figs. 5 and 6, respectively. One can note again that TPC modes do not recover completely at a power density of 45 MW/cm² in PLA with $\lambda = 1.06 \mu\text{m}$ in contrast to PLA with $\lambda = 0.53 \mu\text{m}$ as shown in Figs. 6(b) and 5(d). In addition to higher power density required for PLA with $\lambda = 1.06 \mu\text{m}$, it should be noted that the threshold power density for recrystallization of silicon implanted with P^+ at $f = 3 \times 10^{14}$ ions/cm² is greater than that of silicon implanted with P^+ at $f = 10^{15}$ ions/cm² for both PLA cases, $\lambda = 0.53$ and $1.06 \mu\text{m}$.

Wavelength dependence of the asymmetry of 520 cm^{-1} line, which exhibits a tail on the low-energy side, is ob-

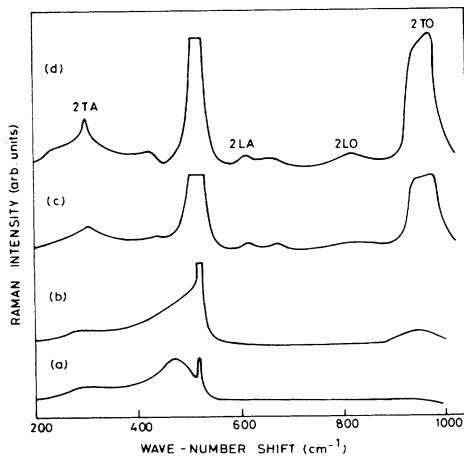


FIG. 5. Room-temperature backscattering Raman spectra with 514.5-nm laser line. (a) Spectrum of silicon implanted with P^+ to a fluence of 10^{15} ions/cm². PLA with $\lambda = 0.53 \mu\text{m}$ is done on same implanted sample using power densities of 21, 35, and 45 MW/cm² in (b), (c), and (d), respectively.

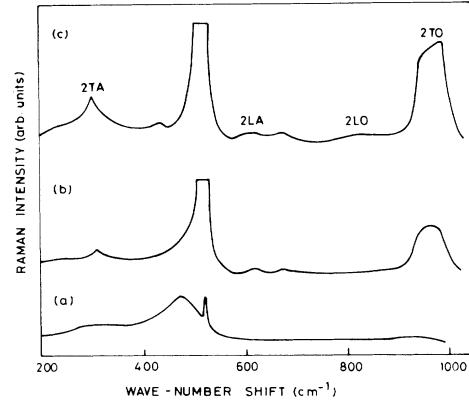


FIG. 6. Room-temperature backscattering Raman spectra with 514.5-nm laser line. (a) Spectrum of silicon sample implanted with P^+ to a fluence of 10^{15} ions/cm². PLA with $\lambda = 1.06 \mu\text{m}$ is done on same implanted sample using power densities of 45 and 55 MW/cm² in (b) and (c), respectively.

served in Figs. 5(d) and 6(c) only when recovery of crystallinity is achieved. Denoting the half-width on low-energy and high-energy sides of the half maximum by Γ_a and Γ_b , respectively, the ratio Γ_a/Γ_b changes from 1 to 1.26 for both Figs. 5(d) and 6(c) as probing laser wavelength is changed from 457 to 514 nm. Figures 3(c) and 4(c) do not show the asymmetry of the one-phonon mode. Asymmetry of the one-phonon mode which is due to the presence of disorder in partially annealed Si as shown in Figs. 3(b), 4(b), 5(b), 5(c), and 6(b), does not show wavelength dependence. It should be noted that one-phonon mode which has been truncated arbitrarily to focus the attention on two-phonon combination modes does not appear completely from Fig. 1 to Fig. 6.

DISCUSSION

Abrupt phase transitions from microcrystalline state to amorphous state has been reported^{8,10} when the grain size of microcrystal is decreased below 30 Å. Interaction between grains seems to stabilize the diamond structure even for small grains ($\sim 30 \text{ Å}$ for silicon). Electron-paramagnetic-resonance experiments¹⁸ have invoked the formation of point defects which form isolated amorphous regions with the increase of fluence in the ion-implantation process. Above the threshold fluence, isolated amorphous layers overlap to produce a continuous amorphous layer. Since Raman scattering is insensitive to point defects, a Raman spectrum of crystalline Si is observed below the threshold fluence. Abrupt phase transitions from *c*-Si to *a*-Si is observed at the threshold fluence when a continuous layer of amorphous phase is formed.

Discontinuity of the coherence length on going from *c*-Si to *a*-Si in Raman spectra requires an excess internal energy and configurational entropy.^{9,19} Free energy of amorphous silicon can be written as

$$F(a\text{-Si}) = E_0 + \delta E(a) - T[S_0 + \delta S(a)], \quad (1)$$

where E_0 and S_0 are molar internal energy and entropy of

crystalline Si, respectively, and $\delta E(a)$ and $\delta S(a)$ stand for the excess configurational internal energy and entropy, respectively. The contribution to free energy due to chemical bonds between species and silicon is neglected because the species after implantation go to interstitial sites which prevent the formation of the bond.

The threshold fluence for an abrupt phase transition can be calculated with thermodynamic arguments using the contribution of kinetic energy of implanted species in nuclear collisions. This contribution increases the free energy of silicon leading to an instability of the diamond structure with respect to amorphous phase. The free energy is so high that the amorphous phase is permitted thermodynamically.^{9,19} Therefore the excess free energy of silicon after ion implantation is directly proportional to the nuclear energy deposited per mole which can be written as

$$F(\text{imp}) = KV_{\text{mole}} \left[\frac{dE}{dx} \right]_{\text{nucl}} f, \quad (2)$$

where K is a constant of proportionality, V_{mole} ($\sim 12 \text{ cm}^3$) the molar volume of solid silicon,⁹ f the fluence of species in ions per square centimeter, and $(dE/dx)_{\text{nucl}}$ the nuclear energy loss in calories per centimeter.

Increasing the free energy with fluence during implantation, the diamond lattice becomes unstable locally (within the microcrystal)^{8,9} with respect to the amorphous phase when the thermodynamic criteria is satisfied using Eqs. (1) and (2)

$$KV_{\text{mole}} \left[\frac{dE}{dx} \right]_{\text{nucl}} f_t = \delta E(a) - T\delta S(a). \quad (3)$$

Since $(dE/dx)_{\text{nucl}}$ is fairly constant for a given energy of implanted species,³ the threshold fluence is only responsible for an abrupt phase transition according to Eq. (3). Variation of $(dE/dx)_{\text{nucl}}$ with energy (E) for a given implanted species^{3,20} is observed to be very small. This is the reason that abrupt phase transition is relatively insensitive to E in comparison with f .¹⁸ The $(dE/dx)_{\text{nucl}}$ is found to increase with the mass of implanted species for its given energy.^{3,20} Therefore the threshold fluence required for an abrupt phase transition decreases with increase of mass of species used in ion implantation process.

$E(a)$ and $S(a)$ (Ref. 9) are $0.1\text{--}0.6 \text{ kcal mol}^{-1}$ and $0.4 \text{ cal K}^{-1} \text{ mol}^{-1}$, respectively, while the threshold fluence (f_t) and $(dE/dx)_{\text{nucl}}$ for P implantation are $5 \times 10^{14} \text{ ions/cm}^2$ in Fig. 1 and $4.7 \times 10^6 \text{ keV/cm}$ ($\sim 1.8 \times 10^{-10} \text{ cal/cm}$),²⁰ respectively. Using these values in Eq. (3), K is found to be 4.43×10^{-4} which is used to calculate the threshold fluence (f_t) of other implanted species given in Table I. This shows excellent agreement between calculated and experimental values of threshold fluence for As^+ and Sb^+ but not for B^+ , for which the Lindhard, Scharff, and Schiott (LSS) theory²¹ fails to determine the exact value of stopping power (S) for light-mass ions.²²

Pulse-laser annealing,^{2,4,12,13,23} which is used to induce the phase change, has been studied at length in recent years. Thermal model of laser annealing¹² based on the rapid transfer of energy from electronic to atomic system

TABLE I. Calculated and experimental threshold fluence of various implanted species in silicon.

Species	(dE/dx) (cal/cm) from Ref. 17	$f_t(\text{calc})$ (ions/cm ²)	$f_t(\text{expt})$ (ions/cm ²)
B	18.43×10^{-12}	4.89×10^{15}	8×10^{16} (Ref. 15)
P	1.8×10^{-10}		5×10^{14}
As	4.63×10^{-10}	1.95×10^{14}	10^{14}
Sb	7.88×10^{-10}	1.1×10^{14}	10^{14} (Ref. 15)

has invoked quick melting at the surface. The transition to a single crystal which is free from extended defects occurs by liquid-phase epitaxy on the crystalline substrate^{12,23} when the melted layer exceeds the thickness of implanted silicon; otherwise there is formation of polycrystalline material on the amorphous layer of implanted Si. One can see the same behavior in Figs. 3, 4, 5, and 6, indicating that there is a threshold power density (ϕ) of PLA to obtain a single crystal. Below the threshold power density, TPC modes in Raman spectra do not recover completely. It has been reported that the threshold power density is directly proportional to X_d , the thickness of amorphous layer²⁴ (i.e., proportional to energy of implant) and decreases exponentially with absorption coefficient (α).²⁵ Hence, threshold power density is

$$\phi_t \propto X_d \exp(-\alpha/A), \quad (4)$$

where A is a constant to be determined from absorption coefficient (α) for which ϕ_t decreases to $(1/e)$ th of the threshold power density required to melt a given thickness (X) of crystalline Si. Equation (4) is only valid when energy absorbed from photons melts a layer of thickness $\sqrt{2D\tau}$ shorter than X_d ,²⁵ D being thermal diffusivity and τ pulse duration. It has been reported²⁵ that ϕ_t increases with the decrease of X_d for $\sqrt{2D\tau}$ greater than X_d .

The absorption coefficient depends upon the coupling of light to disordered material and the degree of disorder, which depends upon temperature during implantation, fluence, and mass of the implanted species. Therefore attention is focused here on the degree of disorder and coupling of light to implanted Si. The degree of disorder is varied by change of fluence from $5 \times 10^{14} \text{ ions/cm}^2$ to $10^{15} \text{ ions/cm}^2$ in Figs. 3, 4, 5, and 6. The ϕ_t is found to decrease with the increase of fluence, in agreement with the fact that absorption coefficient^{24–26} increases with disorder, i.e., low ϕ_t is required to melt the same thickness of highly disordered silicon at lower temperature due to higher free energy.²⁷

The ϕ_t of PLA for phase transitions strongly depends upon the coupling of the wavelength of laser light to implanted material. Photon absorption takes place by the free carrier absorption in the conduction band and by the excitation of valence electrons across the band gap. Photon energy of Nd:YAG laser ($\lambda = 1.06 \mu\text{m}$ and 1.1 eV) marginally exceeds the absorption edge of crystalline silicon and its absorption coefficient is a strong function of temperature, doping density, and defect concentrations.²⁶ Since the photon energy of the second harmonic

($\lambda=0.53 \mu\text{m}$ and $E=2.33 \text{ eV}$) exceeds the absorption edge of crystalline silicon, the absorption coefficient of $\lambda=0.53 \mu\text{m}$ is greater than that of $\lambda=1.06 \mu\text{m}$.²⁶ Therefore one can see in Figs. 3, 4, 5, and 6 that the ϕ , required to melt the same thickness of implanted material is higher for $\lambda=1.06 \mu\text{m}$ in comparison with $\lambda=0.53 \mu\text{m}$.

Asymmetry of ZCP mode in heavily doped n -type Si due to the Fano interaction has been studied at length^{4,28-31} and shows considerable wavelength dependence. This interaction between phonon discrete state and inter-conduction-band electronic (continuum) excitations is observed in Figs. 5(d) and 6(c) when carrier concentrations exceed $10^{19}/\text{cm}^3$. Figures 3(c) and 4(c) of annealed Si do not show asymmetry of the ZCP mode for a fluence of 10^{14} ions/ cm^2 indicating carrier concentration less than $10^{19}/\text{cm}^3$. Line-shape asymmetry of ZCP mode due to the presence of disorder is not expected to show any wavelength dependence.

CONCLUSION

In the present work, we have reported an abrupt phase transition from c -Si to a -Si during the ion-implantation process as the fluence is increased beyond its threshold

value. Threshold fluence required for abrupt phase transitions decreases with the increase of mass of species used in the ion-implantation process. Increase of free energy due to the deposition of kinetic energy of implanted species in nuclear collisions leads to an instability of the diamond structure with respect to amorphous phase.

Systematic investigation of pulsed Nd:YAG laser annealing of silicon implanted with phosphorous ions is also reported here. Transition from amorphous to single crystal occurs above a threshold power density which depends upon absorption coefficient α for a given thickness of implanted Si. Absorption coefficient determines the coupling of light to implanted material and is dependent upon the degree of disorder present in implanted Si. Low-threshold power density is required for highly disordered Si and for smaller wavelength used in pulse-laser annealing.

ACKNOWLEDGMENT

Thanks are due to Dr. W. S. Khokle, Deputy Director, Central Electronics Engineering Research Institute (CEERI), Pilani, for allowing the use of the ion-implantation facilities.

¹See for example, *Ion Implantation and Beam Processing*, edited by J. S. Williams and J. M. Poate (Academic, New York, 1984).

²See for example, *Laser and Electron Beam Processing of Materials*, edited by C. W. White (Academic, New York, 1980).

³K. P. Jain, A. K. Shukla, R. Ashoken, S. C. Abbi, and M. Balkanski, *Phys. Rev. B* **32**, 6688 (1985).

⁴K. P. Jain, A. K. Shukla, S. C. Abbi, and M. Balkanski, *Phys. Rev. B* **32**, 5464 (1985).

⁵M. H. Brodsky, M. Cardona, and J. C. Cuomo, *Phys. Rev. B* **16**, 3556 (1977).

⁶J. E. Smith, Jr., M. H. Brodsky, B. L. Crowder, and M. I. Nathan, *Phys. Rev. Lett.* **26**, 642 (1971).

⁷T. Kamiya, M. Kishi, A. Ushirakawa, and T. Katoda, *Appl. Phys. Lett.* **38**, 377 (1981).

⁸Z. Iqbal and S. Veprek, *J. Phys. C* **15**, 377 (1982).

⁹S. Upprek, Z. Iqbal, and F. A. Sarott, *Philos. Mag. B* **45**, 137 (1982).

¹⁰S. Hayashi, M. Ito, and H. Kanamori, *Solid State Commun.* **44**, 75 (1982).

¹¹R. Shuker and R. W. Gammon, *Phys. Rev. Lett.* **25**, 222 (1970).

¹²P. Baeri, S. U. Campisano, G. Foti, and E. Rimini, *J. Appl. Phys.* **50**, 788 (1979).

¹³C. K. Celler, J. M. Poate, and L. C. Kimerling, *Appl. Phys. Lett.* **32**, 464 (1978).

¹⁴P. Parayanthal and F. H. Polak, *Phys. Rev. Lett.* **52**, 1822 (1984).

¹⁵K. K. Tiong, P. M. Amritharaj, and F. H. Polak, *Appl. Phys. Lett.* **44**, 122 (1984).

¹⁶M. Tsicher, R. Beserman, M. V. Klein, and M. Morkoc, *Phys. Rev. B* **29**, 4652 (1984).

¹⁷D. Bermejo and M. Cardona, *J. Non-Cryst. Solids* **32**, 405 (1979).

¹⁸F. F. Morehead, B. L. Crowder, and R. S. Title, *J. Appl. Phys.* **43**, 1112 (1972).

¹⁹D. Turnbull and D. E. Polk, *J. Non-Cryst. Solids* **8-10**, 19

(1972).

²⁰J. F. Gibbons, William S. Johnson, and Steven W. Mylroie, *Projected Range Statistics*, 2nd ed. (Dowden, Hutchinsons and Ross, Stroudsburg, Pennsylvania, 1975).

²¹G. Carter and W. A. Grant, *Ion Implantation of Semiconductors* (Pitman, London, 1976), p. 2.

²²W. K. Hofher, H. W. Werner, D. P. Oosthoek, and H. A. M. de Grefte, in *Ion Implantation in Semiconductors and other Materials*, edited by Billy L. Crowder (Plenum, New York, 1973), pp. 133-144; David K. Brice, *ibid.* pp. 171-192; Seiji Furukawa and Hideki Matsumura, *ibid.* pp. 193-202.

²³B. C. Larson, *Comments Solid State Phys.* **11**, 151 (1984).

²⁴Dick Hoonhout and Frans Saris, in *Laser and Electron-Beam Solid Interactions and Material Processing*, edited by J. F. Gibbons, L. D. Hess, and T. W. Sigmon (Elsevier/North-Holland, New York, 1981), p. 31.

²⁵P. Baeri, A. E. Barbarino, S. U. Campisano, M. G. Grimuld, G. Foti, and E. Rimini, in *Laser and Electron-Beam Interactions with Solids*, edited by B. R. Appletten and G. K. Celler (Elsevier, New York, 1982), p. 227.

²⁶W. L. Brown, in *Materials Processing Theory and Practices*, edited by M. Bass (North-Holland, New York, 1983), Vol. 2, pp. 341-345.

²⁷*Laser and Electron-Beam Processing of Materials*, edited by C. W. White and P. S. Peerey (Academic, New York, 1980), p. 23.

²⁸G. Contreras, A. K. Sood, M. Cardona, and A. Compaan, *Solid State Commun.* **49**, 303 (1984).

²⁹M. Chandrasekhar, J. B. Renucci, and M. Cardona, *Phys. Rev. B* **17**, 1673 (1978).

³⁰M. Jouanne, R. Beserman, I. Ipatova, and A. Subashiev, *Solid State Commun.* **16**, 1047 (1975).

³¹M. Jouanne, M. A. Kanehisha, J. F. Morhange, N. M. Ravindra, and M. Balkanski, in *Proceedings of the International Conference on Heavy Doping and the Metal-Insulator Transition in Semiconductors*, Santa Cruz, California, 1984 (unpublished).